Critical currents and critical fields in composite Al-Ge films

1994 J. Phys.: Condens. Matter 6 7993

(http://iopscience.iop.org/0953-8984/6/39/019)

J. Phys.: Condens. Matter 6 (1994) 7993–8014. Printed in the UK

Critical currents and critical fields in composite Al–Ge films

Yinon Ashkenazy†, Ralph Rosenbaum† and David Stroud‡

† Tel Aviv University, School of Physics and Astronomy, Raymond and Beverly Sackler Faculty of Exact Sciences, Ramat Aviv 69978, Israel

‡ The Ohio State University, Department of Physics, 174 West 18th Avenue, Columbus, OH 43210, USA

Received 19 January 1994, in final form 15 April 1994

Abstract. Lee and Stroud have predicted that the critical current $I_c(B)$ in a composite superconducting material should display a constant value in moderately high magnetic fields, giving rise to a 'plateau region'. Critical current measurements on granular metallic Al–Ge films, located considerably above the metal–insulator transition (MIT), display well defined plateaus, and these measurements confirm most of the Lee–Stroud predictions. In contrast, films located just above the MIT exhibit continuously decreasing critical currents with increasing magnetic fields. These results are explained using a tunnelling junction model proposed by Peterson and Ekin and extended by Papa and Altshuler. From the fitting results, a simple picture, involving both models, emerges, which explains the behaviour of I_c versus magnetic field in pressed powdered YBCO samples and in Ag-sheathed Bi-based HTC wires, as well as in the Al–Ge films.

1. Introduction

Measurements of the critical current density, J_c, as a function of magnetic field have been made on many superconductors over the past two decades [1, 2]. Many of the results have been interpreted by flux flow and flux creep models [3, 4]. Recently, there is much renewed interest in the J_c versus B properties in the high-temperature superconductors. Some of the first detailed measurements of J_c on bulk sintered samples of powdered YBCO were made by Ekin and co-workers [5–7]. A large decrease of two orders of magnitude in J_c at very low fields (10^{-4}–10^{-2} T) were observed at 76 K (where $t = T/T_c \simeq 0.90$ with $T_c = 85$ K). These results have lead to the suggestion by Ekin and co-workers that the very low J_c values are a result of Josephson weak-link effects in the low-field regime [5, 6]. Peterson and Ekin proposed a model in which different Josephson junction lengths are averaged to account for the interference of the J_c patterns from different junctions [5]. This model was modified and exploited by Papa and Altshuler to fit their YBCO data [8]. Interestingly, we note that the J_c versus B data taken at 4 K (where $t = T/T_c \simeq 0.05$) on YBCO by Ekin and co-workers are very different from the J_c data taken at 76 K [6]. The J_c data at 4.2 K exhibited well defined plateaus of constant magnitude extending from 0.1 T up to 10 T, their largest measuring field. No explanation was given for the origin of the plateaus. The value of J_c in the plateau region was a factor of about ten smaller than the J_c value in zero field. The transition from the 'plateau behaviour' of J_c found at low temperatures to the 'continuously decreasing behaviour' of J_c observed at temperatures close to T_c is well illustrated in figure 8 of [6] for the sintered YBCO samples.

More recently, Sato *et al* have made critical current density measurements on Ag-sheathed BiPbSrCaCuO (the Bi2223 phase) high-temperature superconducting material

0953-8984/94/397993+22$19.50

having $T_c = 110$ K [9]. Sato *et al* observed a large, impressive plateau of constant critical current density J_c at 77 K where $t \simeq 0.70$. The plateau of constant current density started at a magnetic field of 3 T and extended up to their largest available experimental field of 23 T. The magnitude of the critical current density J_c in the plateau region was again about a factor of ten smaller than the zero-field J_c value. Sato *et al* did not study the plateau region as a function of temperature nor of volume fraction ϕ of the superconducting component [9].

In order to explain the critical current density results of Sato *et al*, Lee and Stroud have recently predicted properties for the critical current densities in composite superconducting materials, composed of a superconducting component having a volume fraction ϕ and of a normal metallic component having a volume fraction $1 - \phi$ [10]. These authors suggested that near the metal–insulator transition (MIT) or percolation threshold, the critical current density initially decreases with field and then saturates at a constant value, producing a 'plateau region' with increasing magnetic field. Moreover, in a random but multiply connected network of a strongly linked superconductor, random frustration would produce a plateau in strong magnetic fields. Thus, according to Lee and Stroud, plateaus of constant critical current density should be observed in a wide range of metallic composite films located above the MIT [10].

Motivated by the Lee–Stroud predictions, we made measurements of critical current densities J_c and critical magnetic fields B_c on a completely different composite system—the granular Al–Ge system, where the Al is the superconducting metallic component and the Ge is the insulating component (replacing the Ag normal component). We have recently studied several series of thin 2000 Å granular Al–Ge films, identifying the MIT in each series [11, 12]. This study involves only the metallic films located above the MIT. Since the Al becomes superconducting around 1.6 K in these Al–Ge films and because the superconductivity of the very small clusters and filaments of Al could be completely quenched by a relatively small applied magnetic field of 3.5 T (in contrast with YBCO and the Bi2223 phase), the predictions of the plateau region made by Lee and Stroud could be checked relatively easily by cooling these films in a simple ^{3}He adsorption refrigerator equipped with a small superconducting magnet. These measurements yielded partial confirmation of the Lee–Stroud theory and some unexpected results, too.

This paper is divided into several parts, including summaries of the Peterson–Ekin theory and of the Lee–Stroud theory, a section describing sample and measurement details, and a concluding section that compares experimental results with various different theories.

2. The weak-link models of Peterson and Ekin and of Papa and Altshuler

Peterson and Ekin modelled the YBCO ceramic as a collection of superconducting grains interconnected by weak links, represented by tunnelling junctions, which show a statistical distribution over junction lengths and over orientations of the junction faces relative to the external magnetic field [5]. The dependence of the critical current density upon a magnetic field oriented parallel to the faces of a tunnelling junction is given by the Fraunhofer diffraction formula [13, 4]:

$$J_c(B) = J_0 \sin(\pi\Phi/\Phi_0)/(\pi\Phi/\Phi_0) \tag{1}$$

where the flux quantum $\Phi_0 = h/2e = 2 \times 10^{-15}$ Weber, $\Phi = BL[2\lambda_L(T) + d]$ with B the applied field component normal to the cross sectional area of the junction, L the length

of one tunnelling junction, $\lambda_L(T)$ the London magnetic field penetration depth, and d the thickness of the dielectric layer that separates the two superconducting parallel faces of the tunnel junction. Note that the cross sectional area A_{tj} of the tunnel junction is given by $A_{tj} = L[2\lambda_L(T) + d]$. The prefactor J_0 for a tunnel junction composed of two identical superconducting faces was derived by Ambegaokar and Baratoff [14]:

$$J_0(T) = [\pi \Delta_0(T)/2eR_n] \tanh(\Delta_0(T)/2k_BT) \tag{2}$$

where $\Delta_0(T)$ is the BCS energy gap and R_n is the tunnelling resistance per unit area of the junction when both metals are in the normal state.

In the Peterson–Ekin model, each tunnel junction, having its own specific length L, will pass a current density according to its own Fraunhofer pattern, and interference or summation among these patterns from many different junctions will smear out the J_c versus B pattern [5]. These authors averaged over different lengths L using rectangular, triangular, and skewed Gaussian probability distributions for the random lengths. Each statistical distribution involves two or three fitting parameters including the mean value and the width of the distribution for the lengths.

Several important results were observed by Peterson and Ekin and co-workers [5–7].

(i) The fitting results were found to be relatively insensitive to the type of distribution and the widths of the distribution over a reasonable range of widths.

(ii) For widths greater than about 50% of the mean of the distribution, the Fraunhofer structure became indistinct (that is, J_c became a decreasing monotonic function of increasing magnetic field).

(iii) The calculations showed that the effective critical current density of such a collection of junctions is nearly independent of magnetic field at very low field values.

(iv) The critical current density starts to rapidly decrease at about $B_0/3$, where B_0 corresponds to the first zero in the Fraunhofer diffraction pattern. B_0 is given by $B_0 = \Phi_0/A_{tj}$.

Ekin and co-workers concluded that the rapid decrease in J_c at low fields is a result of weak-link behaviour associated with the tunnel junctions and that the tunnel junctions are located at grain boundaries in powdered YBCO [5–7]. They ruled out flux creep and flux flow mechanisms based upon the observation that J_c was independent of magnetic field orientation with respect to the current direction [5–7].

Papa and Altshuler adapted the Peterson–Ekin model but simplified the averaging procedure [8]. (1) can be written in the form

$$J_c(B) = J_0 \sin(\pi B/B_0)/(\pi B/B_0) \tag{3}$$

where

$$B_0 = \Phi_0/A_{tj} = \Phi_0/[L(2\lambda_L(T) + d]. \tag{4}$$

B_0 is a characteristic field describing one particular tunnelling junction. B_0 depends not only on the geometric character length L of the junction but also on the London penetration depth $\lambda_L(T)$. Thus, Papa and Altshuler obtained the following expression for $J_c(B)$ [8]:

$$J_c(B) = J_0 \int_{B_{min}}^{B_{max}} P(B_0) \frac{\sin(\pi B/B_0)}{\pi B/B_0} \, dB_0 \tag{5}$$

where $P(B_0)$ is the distribution function for the different junction fields B_0. $P(B_0)$ is normalized to unity. The averaging procedure suggested by Papa and Altshuler is conceptually simpler than that of Peterson and Ekin; it gave excellent fits to their J_c versus B data using three fitting parameters [8].

3. Predictions of the Lee–Stroud model

The Lee–Stroud model starts with an ordered simple cubic lattice of resistivity shunted Josephson junctions such that the critical currents I_c and shunt resistances R_0 are all equal [10]. Their percolation structure is depicted in terms of a 'nodes–links' model, in which superconducting chains or links have a typical mean length $L = \xi_p$, which connect one node to another. The links contain Josephson junctions. Here ξ_p is the percolation correlation length (sometimes denoted as the self-similarity length [15]) given by the three-dimensional expression [16–18]

$$\xi_p = d/(\phi - \phi_c)^{0.89} \tag{6}$$

where d is a typical grain diameter. A typical Al grain diameter d is 150 Å for metallic Al–Ge films just above ϕ_c. Note that for a metallic film very close to the MIT, ξ_p diverges to infinite and thus the area, A_{loop}, enclosed by the links of the loop, also diverges. There is no temperature dependence associated with ξ_p.

The key idea of Lee and Stroud is randomness of the areas A_{loop} of the loops [10]. This is equivalent to random displacements of the node locations, in contrast to the perfect ordered rigid cubic lattice arrangement. Let us assume that the actual length of the link, L, is given by a normalized distribution having a mean length of ξ_p and a width σ which is a sizeable fraction of ξ_p. For example if the width σ is large and of the order of 30% of ξ_p, then a typical length of a link could be smaller than 70% of ξ_p or larger than 130% of ξ_p. This would lead to areas (enclosed by the links) that could vary by as much as a factor of four in size from loop to loop. The flux through the αth loop is

$$\Phi_\alpha = BA_\alpha = BL_\alpha^2 \simeq B\xi_p^2. \tag{7}$$

Now introduce f_α, the flux through this loop in units of the superconducting flux quantum $\Phi_0 = h/2e = 2.07 \times 10^{-15}$ J s C^{-1} (T m^2):

$$f_\alpha = \Phi_\alpha/\Phi_0 = BL_\alpha^2/\Phi_0. \tag{8}$$

The f_α can always be written as a sum of an integer n and a fractional part δf_α, which is defined as the frustration. By definition, $0 \leqslant \delta f \leqslant 1$. At zero magnetic field, the frustration, δf, is zero in all the loops, leading to a large critical current $I_c(B = 0)$ through the composite material. The decrease of I_c in small magnetic fields results from the interference of different current patterns from all the different loops. If the loops have random areas and are randomly oriented with respect to the applied field, then at a sufficiently strong field, the frustration will be approximately uniformly distributed between zero and unity, owing to the wide distribution of the effective areas normal to the applied magnetic field. Further increases in the magnetic field, above a certain value, which we designate as the crossover field or beginning field and denote by the symbol B_{beg} (Lee and Stroud use the symbol B_x instead), will not change the distribution of the frustration parameter, and thus the field will not affect the critical current. Thus, for magnetic fields greater than B_{beg}, there should be a plateau of constant critical current.

The plateau of constant current will persist until the magnetic field is so strong that it begins to quench the superconductivity in the larger-diameter links that form the loops. Thus, at fields equal or greater than the critical field of the links, which we denote as B_{end}, Lee and Stroud predict that the critical current will again fall rapidly to zero [10].

We would aniticipate that this 'ending' or terminating field, B_{end}, would be proportional to the upper critical field of the composite material, B_{c2}. Since the upper critical field is temperature dependent near T_c and falls to zero near T_c, we would predict that the 'length' of the plateau, measured in terms of $B_{end} - B_{beg}$, will become shorter as the experimental temperature approaches T_c. At temperatures sufficiently close to T_c, we would predict that B_{end} would merge upon B_{beg}, and, hence, we would not expect to observe a plateau region.

The temperature dependence of the upper critical field B_{c2} in a dirty type-II superconductor has a $B_{c2} \propto 1/\xi_s^2 \propto (1-t)^1$ dependence, where ξ_s is the superconducting coherence length and $t = T/T_c$ [4, 19]. In contrast, the temperature dependence of the critical field in a percolation structure goes as $B_{end} \propto (1-t)^{0.53}$ according to Alexander [20]. Thus, the value of the exponent describing the critical field data B_{end} should give some indication of the morphology of the films.

We now present a qualitative argument of Lee and Stroud to estimate the crossover field, B_{beg}, where the plateau first begins, after the initial decrease of the critical current in small fields [10]. The flux through a given loop is $\Phi = BA_{loop}$. Hence, the RMS fluctuation in the flux is $\Delta\Phi = B\Delta A_{loop}$, where ΔA_{loop} is the RMS fluctuation of the loop areas. The frustration in the loop is $\delta f = \Delta\Phi/\Phi_0$. Hence the RMS fluctuation in the frustration is $\Delta f = B\Delta A_{loop}/\Phi_0$. When this is of the order of unity, further increases in the field will not change the distribution in this frustration; hence, the critical current should become field independent. The condition that $\Delta f = 1$ is equivalent to

$$B_{beg} = \Phi_0/\Delta A_{loop}. \tag{9}$$

In terms of the characteristic field $B_0 = \Phi_0/A$ from (4), the above equation becomes

$$B_{beg} \simeq B_0^2/\Delta B_0 \tag{10}$$

where ΔB_0 is the RMS fluctuation (or spread) in the characteristic field.

Since the percolation correlation length ξ_p diverges near the MIT, the crossover field is predicted to decrease to zero for samples located near the MIT, going as $B_{beg} \propto 1/A_{loop} \propto \xi_p^{-2} \propto (\phi - \phi_c)^{1.78}$. Note that the crossover field has no temperature dependence if the field penetration into the links that form a loop is neglected. If the field penetration is included, the loop area becomes temperature dependent:

$$A_{loop} = [\xi_p + 2\lambda_L(T)]^2. \tag{11}$$

We approximate the RMS fluctuation of the loop areas, ΔA_{loop}, with the average loop area by substituting (11) into (9) to yield an estimation for B_{beg}:

$$B_{beg} \simeq \Phi_0/[\xi_p + 2\lambda_L(T)]^2 \tag{12}$$

where $\lambda_L(T)$ is the London penetration depth approximated by the Ginzberg–Landau expression $\lambda_L(T) = \lambda_L(0)/(1-t)^{1/2}$ with $\lambda_L(0) = 500$ Å for bulk Al [14, 19]. The Ginzburg–Landau expression is also valid for percolating clusters in the homogeneous regime where the film thickness is larger than ξ_p [37].

Summarizing, we note that the beginning field B_{beg} is the minimum magnetic field that causes the flux in the smallest loops to exceed the flux quantum Φ_0. All the other larger loops have fluxes that exceed Φ_0. When the given applied field is equal to B_{beg}, there will be a particular current distribution throughout all the loops. If we now change the applied field to a new value that exceeds B_{beg}, the overall current distribution throughout

the loops will not change owing to the broad spread (or randomness) in the loop areas and to the periodicity of the current with Φ_0. The current magnitude in a particular loop will change with applied field, but the total number of loops throughout the sample that carry a particular current value will not change with applied field. Thus, the overall current transported throughout all the loops remain the same for all fields exceeding B_{beg}, thus giving rise to the plateau.

We extend the frustration argument of Lee and Stroud to the case of tunnelling junctions rather than that of superconducting loops. In the case of junctions, (9) becomes

$$B_{beg} = \Phi_0/\Delta A_{tj} \tag{13}$$

where ΔA_{tj} is the width or the standard deviation in the cross sectional areas of the junctions owing to randomness. In this case, B_{beg} is a characteristic field that separates the rapidly decreasing region of I_c in small fields from the relatively weak $J_c \propto 1/B$ dependence at moderate fields. The motivation for using (13) is that a temperature dependence is again introduced into B_{beg} via $\Delta A_{tj} = [d + 2\lambda_L(T)]\,\Delta L$.

We summarize three other relevant predictions from the Lee–Stroud paper [10].

(i) The magnitude of the current in the plateau region is about 10% of the zero-field current value; that is, $J_c(p)/J_c(B = 0) \simeq 0.1$.

(ii) The fractional decrease of the critical current density should follow the relation $1 - J_c(p)/J_c(B = 0) \propto 1/\xi_p^2 \propto (\phi - \phi_c)^{1.78}$.

(iii) The critical current density in zero field, $J_c(0)$, should scale with the metal content ϕ as $J_c(\phi) \propto 1/\xi_p^2 \propto (\phi - \phi_c)^{1.78}$. This result is consistent with the predictions of Kirkpatrick and of Deutscher and Rappaport [21, 22] that $J_c(\phi) \propto (\phi - \phi_c)^{(D-1)\gamma}$. Here D is the dimensionality of the sample and γ is the critical index of the percolation correlation length ξ_p ($\gamma \simeq 0.89$ in $D = 3$ and $\gamma \simeq 1.3$ in $D = 2$) [16, 18].

We now illustrate the evolution of the plateau with increasing randomness in the loop areas using our own very simple model. We follow the approaches of Peterson and Ekin and of Papa and Altshuler in calculating the critical current I_c versus B [5, 8]. However, we replace the expression $\sin(x)/x$ describing the tunnel junction by a simple $\cos(x)$ function describing a superconducting loop interrupted by a Josephson junction. Assume that a superconducting loop encloses an area A_{loop} and contains a total of N Josephson junctions. The maximum critical current is given by

$$I_{c,max} = 2I_0 \cos(2\pi\Phi/N\Phi_0) = 2I_0 \cos(\pi B/B_0) \tag{14}$$

where

$$B_0 = N\Phi_0/2A_{loop}. \tag{15}$$

For the special case of the DC SQUID structure having one weak link in each half loop, (14) simplifies to the well known relation that $I_{c,max} = 2I_0 \cos(\pi\Phi/\Phi_0)$. Assuming that our sample is composed of many loops enclosing different areas, we average (14) over all the areas to estimate the J_c versus B behaviour for the sample:

$$J_c(B) = J_c(0) \int_{B_{min}}^{B_{max}} P(B_0) \cos(\pi B/B_0)\, dB_0. \tag{16}$$

Based upon the claim that the averages are relatively insensitive to the type of distribution function $P(B_0)$ selected, we have chosen the normalized skewed triangular

distribution function. Three fitting parameters are used to describe the triangle: B_{min}, the minimum field for B_0, below which the distribution function is zero, B_{peak}, where the probability reaches its maximum value of $2/(B_{max} - B_{min})$, and B_{max}, above which the distribution is again zero. It is important that B_{min} takes on a finite value for two reasons: the argument of the sine and cosine functions, $\pi B/B_0$, is undefined if B_{min} and hence B_0 are set to zero; and a zero value for B_0 implies an infinite cross sectional area A_{tj} for the tunnelling junction and/or an infinite loop area A_{loop}, which are unphysical cases. Note that the full width of the distribution function is $2\sigma = (B_{max} - B_{min})/2 = 2\Delta B_0$.

Using the skewed triangular distribution for $P(B_0)$, we consider three cases. The first case is of no randomness and where all the loops have identical areas. Hence the distribution function becomes a delta function peaking at $B_0 = B_{peak}$, $P(B_0) = \delta(B_0 - B_{peak})$. For this case $J_c(B)$ is periodic in magnetic field exhibiting a simple $|\cos(x)|$ dependence as shown in figure 1(*a*). The second case is where there is a small amount of randomness in the areas. For this case, we choose $B_{min} = 0.8B_{peak} = 0.08$ T, $B_{peak} = 0.1$ T, and $B_{max} = 1.2B_{peak} = 0.12$ T. The averaging results, shown in figure 1(*b*), illustrate that the plateau region develops only at large fields of magnitude $B_{beg} \simeq 4B_{peak}^2/(B_{max} - B_{min})$ according to (10) and converges to a value of $2J_c(0)/\pi$. The width in this case is not so large and of the order of $0.2B_{peak}$. In the last case of strong randomness in the loop areas, we observe a well defined plateau in moderate fields developing after an initial decrease of J_c in small fields, as seen in figure 1(*c*). The curve parameters in this case are $B_{min} = 0.01B_{peak} = 0.001$ T, $B_{peak} = 0.1$ T and $B_{max} = 6B_{peak} = 0.6$ T; thus, the width is $3B_{peak}$. Two important points are observed from figure 1(*c*). A plateau of constant current results from strong randomness of loop areas, as predicted by Lee and Stroud [10] and the magnitude of I_c in the plateau region is only a factor of $2/\pi$ smaller than the zero-field value $J_c(0)$ using our simplified model. Although the Lee–Stroud model nicely predicts the presence of plateaus in moderately strong magnetic fields and decreases of I_c by a factor of ten, our model cannot explain the large initial decrease of I_c we observe experimentally at smaller fields.

4. Sample preparation and measurement techniques

Al–Ge granular films were fabricated by co-evaporating Al and Ge simultaneously using two electron guns. These materials were deposited upon thin glass slices of dimensions 2.5 mm × 25 mm maintained near room temperature in order to obtain the granular structure composed of Al grains coated with amorphous Ge. The glass substrate was intentionally not heated to avoid obtaining the 'random structure' [23, 24]. Each glass slice differs in its Al content from those of its two neighbours by about 2%, with the slice closest to the Al boat having a metal volume fraction ϕ of 63.3% Al in contrast to the slice closest to the Ge boat having a ϕ of 44.4% Al. An EDAX (energy dispersive analysis of x-rays) probe attached to a transmission electron microscope was used to yield the Al volume fractions ϕ. The superconducting properties of the films in an applied magnetic field yielded the critical volume fraction, $\phi_c = 50.7\%$ Al at the MIT for the series 9 to be discussed in this paper [11, 12]. Only the metallic films from series 9, some twelve in number, were used in this study.

Superconducting critical currents were measured using the 1 μV cm^{-1} criterion. This was the smallest voltage change that we could accurately detect. An HP3456 microvoltmeter was used to measure and to average the voltage readings. The background voltage, which arose from thermal EMFs on the voltage leads, was first determined, without application of

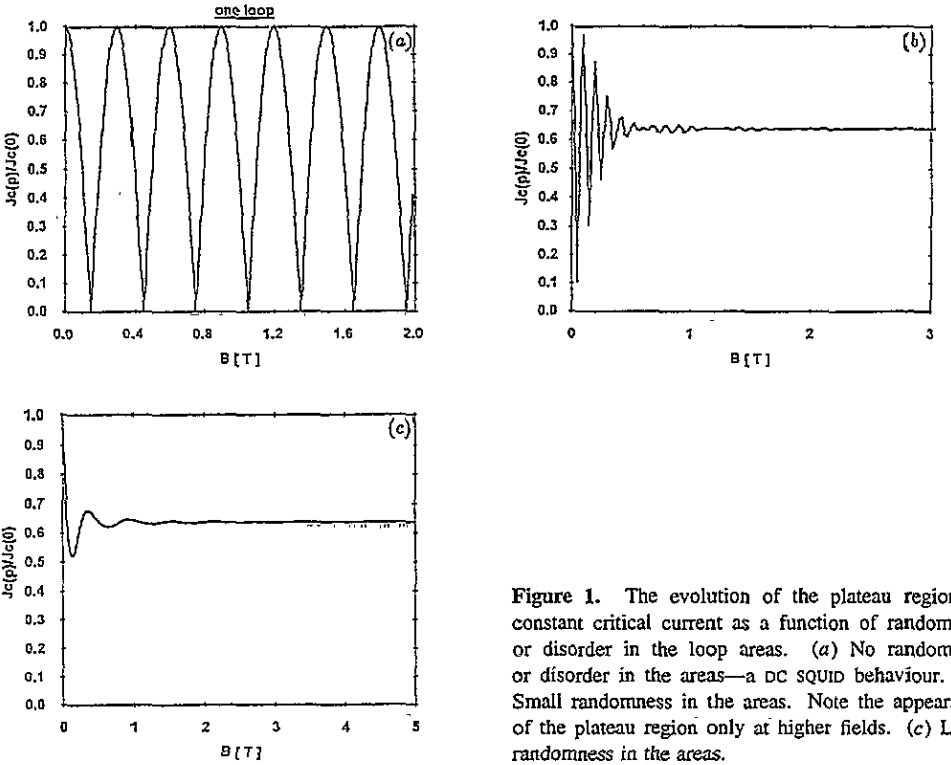

Figure 1. The evolution of the plateau region of constant critical current as a function of randomness or disorder in the loop areas. (*a*) No randomness or disorder in the areas—a DC SQUID behaviour. (*b*) Small randomness in the areas. Note the appearance of the plateau region only at higher fields. (*c*) Large randomness in the areas.

the current to the film. A DC current from a Keithley 224 current source was then applied to the film and varied in magnitude until the 1 μV cm^{-1} difference was observed. This procedure was done at different fixed temperatures below T_c as a function of magnetic field. By careful averaging of the measured voltages, the critical currents could be determined to $\pm 1\%$ accuracy. An alternative criterion was recently suggested by Ekin, in which tangents to the V versus I curves are extrapolated to zero voltages to yield I_c values [25]. No detectable hysteresis in I_c was observed with increasing and with decreasing magnetic fields above 500 G.

Determination of B_{end} where the plateau region 'ends' or 'terminates' was a straightforward procedure. This was the field to first quench some of the superconductivity in the loops and to cause the critical current to first deviate to values lower than the constant value observed in the plateau region. B_{end} is known to $\pm 5\%$.

Determination of the crossover field B_{beg} where the plateau first 'begins' or 'starts' was more difficult. We chose the criterion of the intersection point of two extrapolated lines. One line was passed through the constant-current region of the plateau and extended into the low-field region. The second line was passed through the rapidly decreasing critical current points near the zero-field region and extended to the moderate-field region. The placement of this second line was somewhat arbitrary owing to scatter in the critical current data and this uncertainty led to a large error of $\pm 25\%$ in determining the intersection point and hence the value of the crossover field, B_{beg}.

The upper critical field data were determined using the $\rho_n/2$ criterion where $B_c(T)$ is the critical field that restored the resistivity of the film to one-half of its normal resistivity value of ρ_n at a given temperature $T \leqslant T_c$. Owing to a large superconducting fluctuation contribution to the electrical conductivity in these films above T_c (namely, the Maki–

Thompson and Aslamazov–Larkin terms), B_c does not go to zero at $T = T_c$ as observed in bulk metallic films. The critical fields are of the order of 1.5–3.1 T in these granular Al–Ge films, and are greatly enhanced over the small critical field of 0.01 T observed in bulk Al. This enhancement arises from the very small dimensions associated with Al clusters and grains, as was predicted by Douglass [26]. Fortunately, a 3.5 T field was sufficient to completely quench all superconductivity in the films of this series 9.

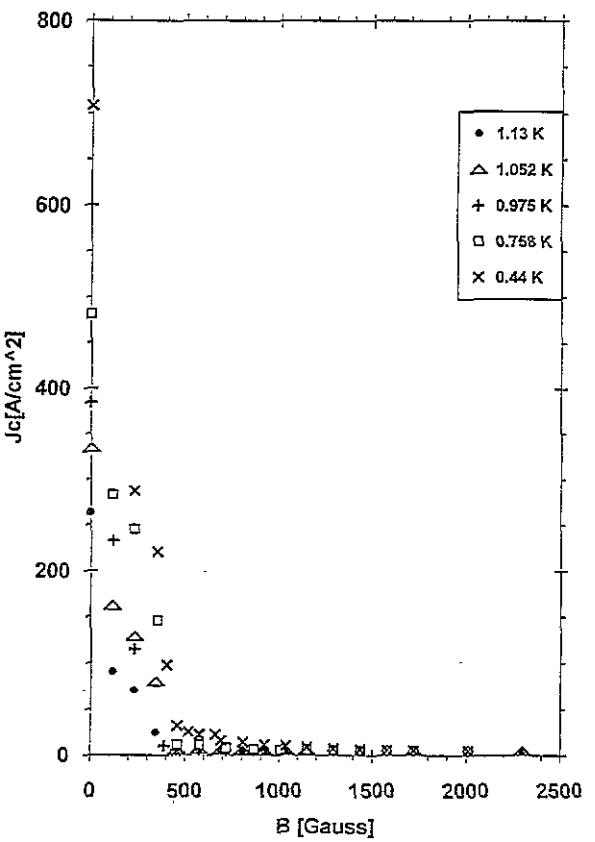

Figure 2. The low-field behaviour of the critical current density for the very metallic 62.4% Al film, as a function of magnetic field at fixed temperatures considerably lower than $T_c = 1.68$ K. It is difficult to detect the plateau regions owing to the vertical and horizontal scales used in this figure. Symbols: filled circles, 1.13 K; empty triangles, 1.052 K; plus signs, 0.975 K; empty squares, 0.758 K; crosses, 0.44 K.

5. Results and comparison with the theories

We had initially anticipated observing plateaus in all the metallic films, but we were quickly surprised to discover that only the most metallic films in series 9, having Al volume fractions $\phi > 58\%$ Al, exhibited plateaus of constant critical currents.

We now present detailed data on the 62.4% Al film. The results on this 62.4% Al film are characteristic and representative of the results observed in the other neighbouring

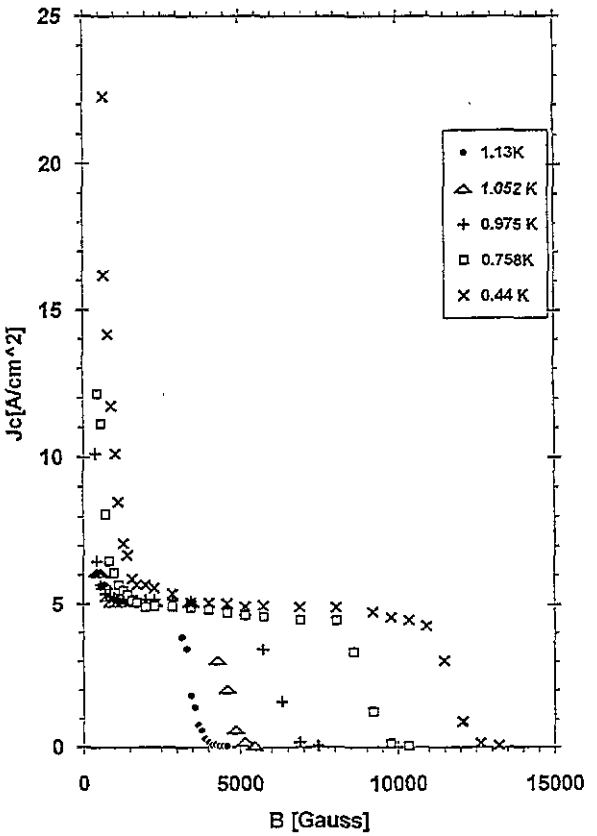

Figure 3. The high-field behaviour of the critical current density for the 62.4% Al film. Here the vertical scale has been expanded by a factor of 30 and the horizontal scale by a factor of five as compared to those of figure 2. This figure clearly demonstrates that there are plateau regions of constant critical current density and that the 'beginning' (crossover) and 'ending' (terminating) fields of the plateaus are temperature dependent, both decreasing to zero with higher temperatures. From these curves, values for the crossover fields can be obtained by interpolation (see text). Symbols: filled circles, 1.13 K; empty triangles, 1.052 K; plus signs, 0.975 K; empty squares, 0.758 K; crosses, 0.44 K.

metallic films and on other very metallic films from other series. This film had a room temperature resistivity of 3.5×10^{-4} Ω cm, a cross sectional area of 4.96×10^{-6} cm^2, and a T_c of 1.667 K.

The dependence of the critical current density $J_c(B, T)$ upon magnetic field at different fixed temperatures is shown in figures 2, 3 and 4. Very well defined plateaus are observed at all temperatures except for the two highest measurement temperatures of $T = 1.33$ K and $T = 1.41$ K, corresponding to reduced temperatures of $t = 0.80$ and $t = 0.85$ respectively. At the highest temperatures B_{end} merges into B_{beg}. From the plateau curves of figures 2, 3, and 4, the crossover field, B_{beg}, and the ending field, B_{end}, were extracted and are shown in figures 5 and 6, respectively. Note that B_{beg} is temperature dependent, as seen from figure 5. The Lee–Stroud theory predicts that B_{beg} should be temperature independent. We also note that the magnitude of the critical current density in the plateau region at the lowest measuring temperature of 0.44 K is a factor of 150 times smaller than the zero-field $J_c(0)$

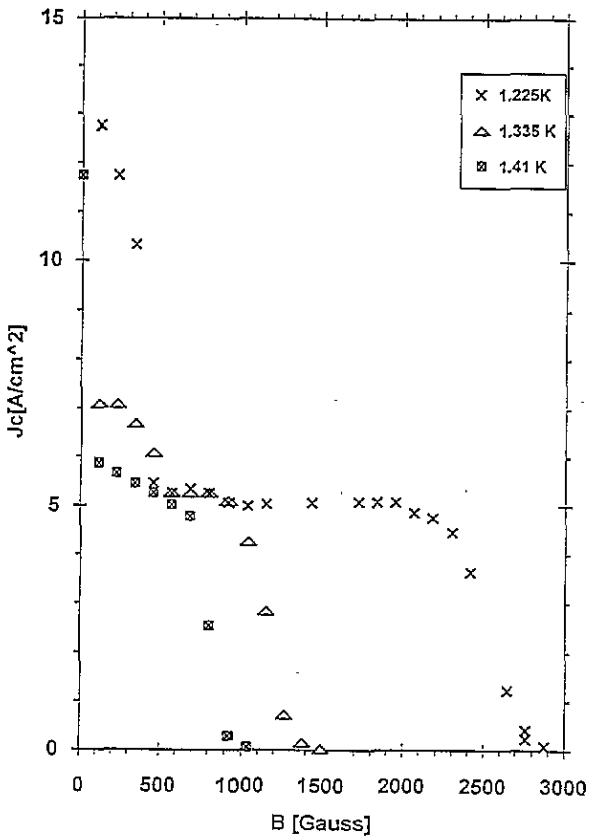

Figure 4. Expanded views of the plateau regions for temperatures slightly below $T_c = 1.68$ K for the 62.4% Al film. Note that the crossover fields and ending fields approach zero as T approaches T_c. There is no indication of a plateau region in the $T = 1.41$ K data ($t = 0.84$) owing to the small value of the 'ending' (terminating) field at this high temperature. Not shown are the zero-field values of $J_c(B = 0)$ at 1.225 K and 1.335 K, which are 111 A cm^{-2} and 30.2 A cm^{-2} respectively. Symbols: crosses, 1.225 K; empty triangles, 1.335 K; crosses in squares, 1.41 K.

value. In addition, the J_c (plateau) appears to be completely temperature independent, and we have no explanation for this behaviour.

Some of the predictions of Lee and Stroud are well verified, such as the existence of well defined plateaus bounded by B_{beg} and B_{end} as seen in figures 2, 3, and 4. Lee and Stroud claim in their concluding remarks that even very metallic samples should exhibit plateaus, as is the case for this 62.4% Al film [10]. Our $J_c(B)$ plateau results are not unique to the Al–Ge composite system. Similar results were reported by Ekin and co-workers in [6] (see figure 8) on bulk sintered samples of powdered YBCO. Although their system is completely different from ours, the general behaviour is the same. Plateaus of constant current appeared only at temperatures lower than 64.3 K corresponding to a reduced temperature of 0.76 for the YBCO samples [6]. Sato *et al* observed well defined plateaus in Ag-sheathed Bi2223 wires at 4.2 K where $t = 0.04$ and even at 77.3 K where $t = 0.70$ [9].

We now propose a simple model that can explain both the initial rapid decrease of J_c in small fields and the constant value of J_c in moderate fields. Consider that the metallic

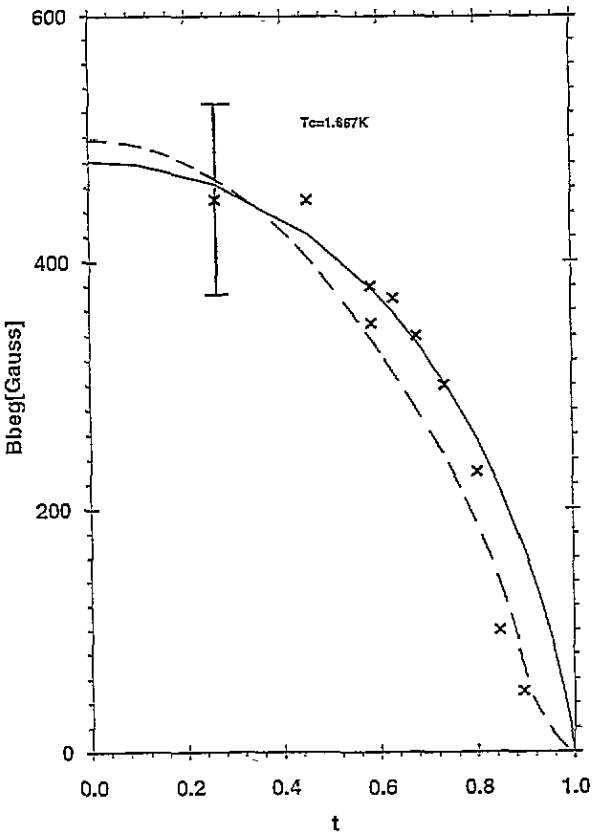

Figure 5. The temperature dependence of the crossover field, B_{beg}, as a function of the reduced temperature $t = T/T_c$ where $T_c = 1.67$ K for the 62.4% Al film. The solid line is the prediction of (12) using the expression $\lambda_L(0)/(1-t)^{1/2}$ for the penetration depth. The dashed line is based upon the thermal energy exceeding the Josephson coupling energy, thus driving Josephson junctions located on the backbones into their normal state; thus, the effective loop areas increase with increasing temperature.

Al–Ge films are connected from end to end by many 'discontinuous' backbones, that is, backbones that are interrupted by weak lines in the form of Josephson tunnelling junctions (TJs) having random cross sectional areas A_{tj} as illustrated in figure 7. The cross sectional area is $A_{tj} = L[d + 2\lambda_L(T)]$, where d is the thickness of the insulating barrier, L is the random length of the junction, and $\lambda_L(T)$ is the London penetration depth. We have fitted the averaged predicted $J_c(B)$ values using (5) of Peterson and Ekin to the $T = 0.44$ K data of the 62.4% Al film. The resulting comparison is shown by line a in figure 8 where the following fitting parameters were used in $P(B_0)$: $B_{min} = 0.00079$ T, $B_{peak} = 0.0019$ T, and $B_{max} = 0.02$ T. Of course, the plateau region is missing, owing to the $1/x$ dependence in the Fraunhofer expression.

We now introduce the Lee–Stroud contribution to the critical current density arising from the behaviour of the random loops. Each backbone has a large number of dangling bonds. Dangling bonds from one backbone are weakly coupled to dangling bonds from neighbouring backbones via Josephson weak links as illustrated in figure 7. Thus, these bonds become the links in the Lee–Stroud model. We thus fit (16) to the plateau region

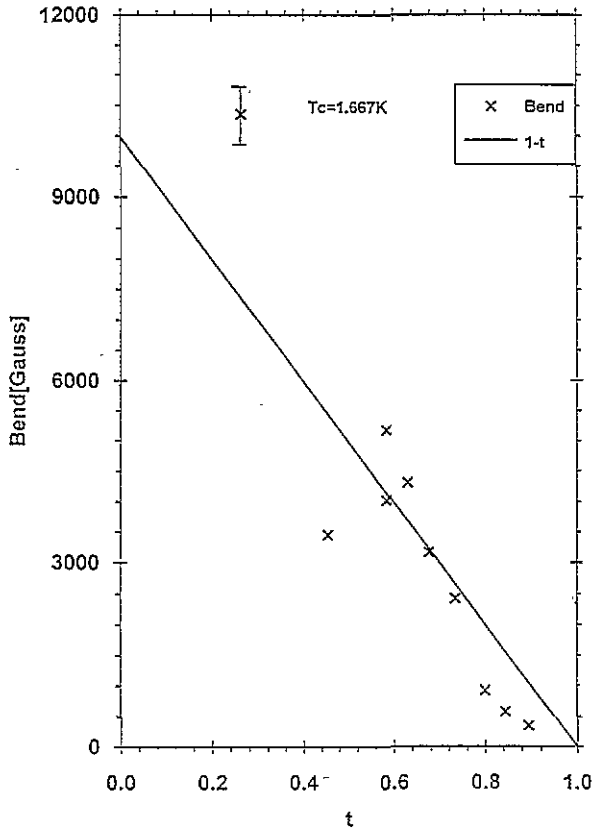

Figure 6. The 'ending' or terminating field, B_{end}, of the plateau region as a function of the reduced temperature $t = T/T_c$ where $T_c = 1.67$ K for the 62.4% Al film. The solid line is a fit using the expression $B_{end}(T) = B_0(1-t)^1$, which describes a type-II dirty superconductor.

using four fitting parameters: $J_c(B=0) = 5.6$ A cm^{-2}, $B_{min} = 0.06$ T, $B_{peak} = 0.16$ T, and $B_{max} = 0.63$ T. However, from figure 1, we observed that the plateau value is $2J_c(0)/\pi$; since we know the plateau magnitude from the experimental results, we also know $J_c(0)$. The fitting results are shown by line b in figure 8. The two contributions, from the tunnelling junctions and from the loops, are now added together to yield the final results that appear as line c in figure 8. The fit to the data is quite acceptable, which is not surprising since six fitting parameters were used. The theory does not take into account the second rapid decrease of J_c when the magnetic field drives the links into the normal state.

There are other models that predict the rapid decreases of $J_c(B)$ with small increasing magnetic fields. In one model, the field generated by a current flowing in a wire and the external applied field can be added together [27]. When this sum exceeds the critical field, the critical current is determined. This is known as Silsbee's theorem [27]. In this model the critical current decreases linearly with applied field; however, we do not observe a linear decrease nor do we obtain a realistic value for the effective diameter of the wire, which appears as a fitting parameter. The second model is based upon flux flow and is known as the Lorentz force-limited behaviour [3,4]; this model predicts that $J_c \propto 1/B$, which can be fitted quite nicely to the intermediate-field data appearing in figure 10. However, this model cannot explain the initial rapid decrease of $J_c(B)$ in small fields. Moreover,

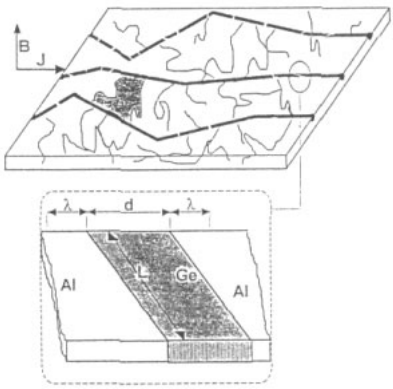

Figure 7. A schematic view of the Al–Ge morphology. The backbones, represented by the wide lines, connect the sample from end to end and carry most of the current in zero field. These backbones are composed of grains joined by metallic contacts and by tunnelling junctions. One of the tunnelling junctions is illustrated in detail with its characteristic sizes. When the magnetic field is applied normal to the current flow, some of the junctions along the backbones start to become normal, and the current is forced to go through the dangling bonds, which provide alternative paths between the backbones. The dangling bonds from varoius backbones are connected to one another via Josephson weak links to form closed loops. In high fields most of the current flows through the loops of the dangling bonds. A plateau of constant critical current results from the randomness in the loop areas. One of these closed loops of random area is marked by the hatchings.

hysteresis would be anticipated. A third model has been proposed by Gerber *et al* [28].

A modified collective pinning theory by Fehrenbacher and co-workers predicts a good qualitative description of the observed J_c versus B behaviour [29]. This paper is based upon earlier important plateau predictions by Vinokur and Koshelev using a collective pinning theory of Larkin and Ovchinnikov [30, 31]. The theory of Fehrenbacher *et al* predicts the initial rapid drop of J_c by a factor of thirty with small B values, a plateau region for intermediate fields and a subsequent second drop of J_c for high B values, as can be seen in their figure 10(d) in [29]. Moreover, they predict a temperature-dependent beginning field given by $H_{co} = \Phi_0/[\pi\lambda_J(2\lambda_L + d)]$, where λ_J is the temperature-dependent Josephson penetration length. Their model is based upon depinning of Josephson vortices at random pinning sites in long Josephson junctions. Their predictions are strictly valid only at $T = 0$ K, using several adjustable fitting parameters. Note, however, that there are a few discrepancies between this theory and our data. Our limited TEM studies suggest that our junctions are 'short'—of the order of 200–1000 Å. In contrast, a long Josephson junction has a length L satisfying $L \gg \lambda_J$. Since λ_J is of the order of a few micrometres, the theory applies to junctions having lengths of the order of ten micrometres. Our morphology does not satisfy this condition. This theory predicts a 'second short' plateau that occurs when the vortex lattice spacing, a, becomes equal to the average pin centre size, r_0. It is not clear from our low-temperature data of figure 3 whether this second plateau is present. More disturbing is the prediction that the second decrease of J_c should fall off slowly with field as $1/B$; our results indicate that J_c falls off much more rapidly to zero, within a factor of three increase of magnetic field (see figures 3, 4 and 10), as compared to several orders of magnitude increase in field as suggested by the theory. Overall, the Fehrenbacher–Geshkenbein–Blatter theory provides an alternative explanation to our results [29].

The beginning field B_{beg} has a definite temperature dependence as seen from figure 5.

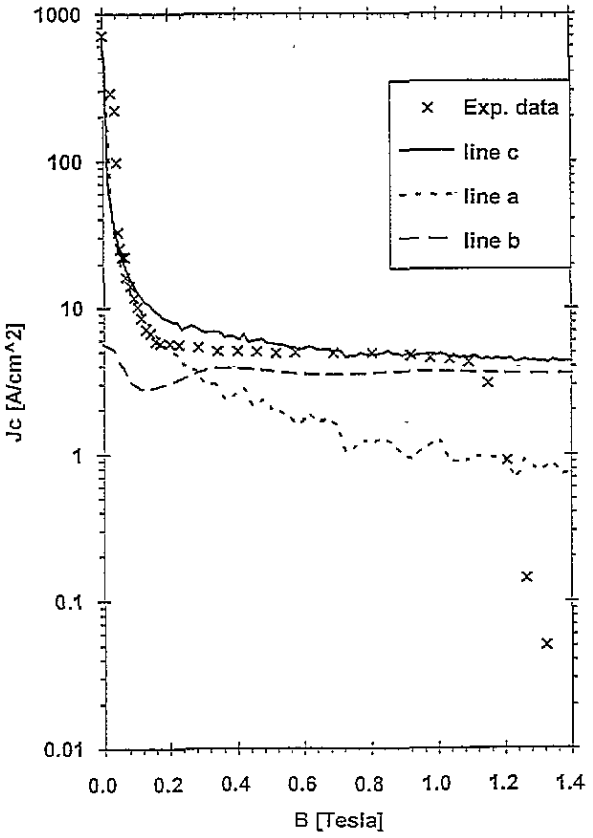

Figure 8. Fits of the Peterson–Ekin theory (line a), the Lee–Stroud theory (line b), and the sum of both contributions (line c) compared to the $J_c(B)$ data for the 62.4% Al film at $T = 0.44$ K. The fitting parameters are given in the text.

Recall that the London penetration depth introduces a temperature dependence into the loop area and hence into the crossover field B_{beg}. Near T_c, B_{beg} should approach zero, as can be seen in figures 4 and 5, since $\lambda_L(T) \to \infty$. The solid line in figure 5 represents B_{beg}, using the Ginzburg–Landau penetration depth expression $\lambda_L(T) = \lambda_L(0)/(1-t)^{1/2}$ in (12); $\lambda_L(0)$ and ξ_p were the only fitting parameters which took on the magnitudes of 500 ± 80 Å and 930 ± 200 Å. The $\lambda_L(0)$ value agrees with the experimental penetration depth value for bulk Al and the ξ_p value agrees with the predicted value of ξ_p using (6) with $d_{grain} = 150$ Å and $\phi_c = 50.7\%$ Al for this 62.4% Al film; for this case $\xi_p = 1010$ Å. A poorer fit was obtained when the Gorter–Casimir expression $\lambda_L(T) = \lambda_L(0)/(1-t^4)^{1/2}$ was used for the penetration depth.

Note, however, that we might be incorrect in using the expression $A = (\xi_p + 2\lambda_L)^2$ to represent the effctive loop area since in our case the magnetic penetration depth λ_L is considerably greater than the diameter d of the small 150 Å Al filaments; in this case the magnetic field penetrates rather uniformly throughout the superconducting filaments at all temperatures. An alternative explanation is needed and is based using Ekin's model where an increasing number of Josephson junctions located on the backbones are driven into the normal state with increasing temperature. As the temperature approaches T_c, the

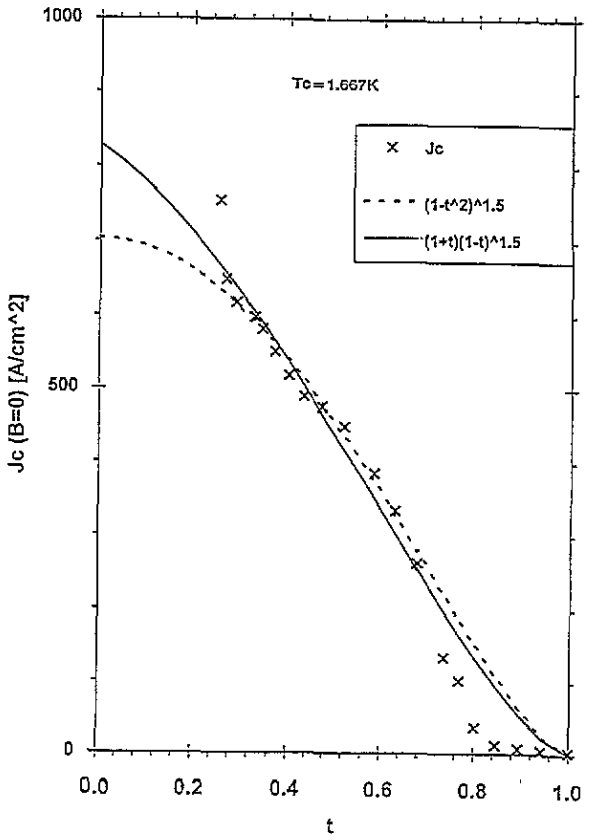

Figure 9. The critical current density $J_c(B = 0)$ at zero magnetic field as a function of reduced temperature $t = T/T_c$ where $T_c = 1.667$ K for the 62.4% Al film. The dashed line is from the Bardeen expression for the critical current of dirty films given by (17), while the solid line is from the Deutscher theory for a granular superconductor having moderate intergrain coupling given by (18). Both fits are good.

Josephson coupling energy $E_J = J_0(T)h/2e$ approaches zero, while in contrast the thermal energy $E_T = k_BT$ increases with increasing temperature. $J_0(T)$ is given by (2) with R_n now representing the resistance per junction in the normal state. When $E_J < E_T$, the junction reverts to the normal state [38], and the supercurrent that was flowing in this previously closed loop must now find a new alternative path that involves a new loop of larger area. Thus, this model also predicts that B_{beg} would tend to zero as $T \to T_c$. An intuitive argument based upon $E_J = J_0(T)h/2e$ would suggest that the effective area would be given by $A = [\xi_p + l_{eff}\Delta(0)/(\Delta(T)\tanh(\Delta(T)/2k_BT))]$ and $B_{beg} \simeq \Phi_0/A$. Setting $\xi_p = l_{eff} = 1000$ Å, the dashed line in figure 5 was obtained, yielding a good fit to the B_{beg} data.

B_{end} exhibited a $(1 - t)^1$ temperature dependence as shown in figure 6; this result suggests that this 62.4% Al film behaves as a dirty type-II superconductor. In addition, B_{c2} also exhibited a $(1 - t)^1$ temperature dependence; B_{c2} had a magnitude twice that of B_{end}.

The critical current density in zero magnetic field, $J_c(B = 0)$, as a function of reduced temperature for the 62.4% Al film appears in figure 9. The temperature dependence can be well described using the Bardeen expression for a dirty type-II superconductor [32]

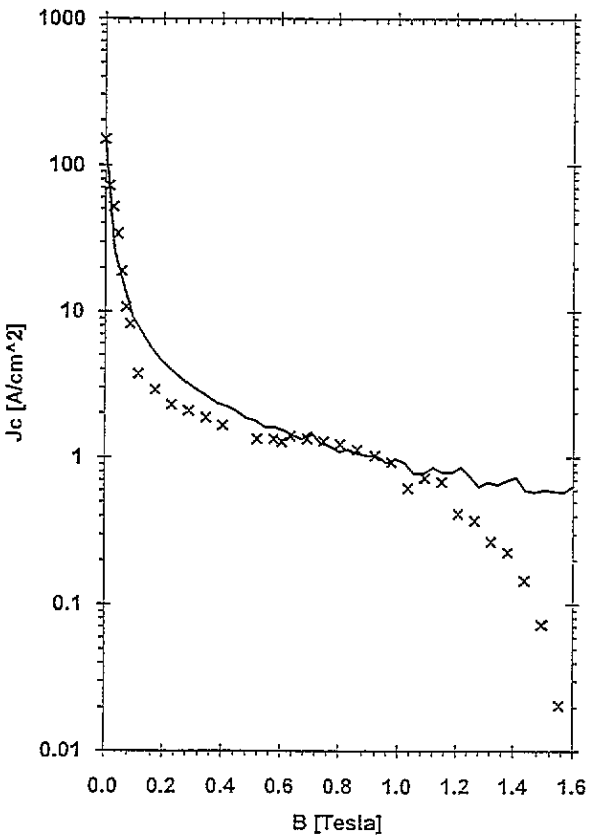

Figure 10. The overall behaviour of the critical current density $J_c(B)$ versus magnetic field for the 51.2% Al film. This film is located just above the MIT ($\phi_c = 50.7\%$ Al) and has a $T_c = 1.28$ K. The data are taken at the fixed temperature of $T = 0.44$ K. There is no plateau region of constant critical current density in this film. The solid line is a fit of the Peterson–Ekin theory to the $J_c(B)$ data for the 51.2% Al film at 0.44 K. The fitting parameters are summarized in the text.

$$J_c(T, B = 0) = J_c(0, 0)(1 - t^2)^{3/2} \tag{17}$$

or the Deutscher expression for moderately strongly coupled grains [33]

$$J_c(T, B = 0) = J_c(0, 0)(1 - t)^{3/2}(1 + t). \tag{18}$$

We had anticipated that the $J_c(B = 0)$ versus t dependence would have been best described by the Ambegaokar–Baratoff equation (2) for tunnelling junctions, which was not the case [14].

We now examine the critical current properties of the 'least' metallic film having $\phi = 51.2\%$ Al. This film was located slightly above the MIT at $\phi_c = 50.7\%$ Al. This film has a resistivity of 9.6×10^{-3} Ω cm, a cross sectional area of 4.86×10^{-6} cm^2, and a T_c of 1.28 K. The data of this film are characteristic of the other metallic films located close to the MIT.

The overall behaviour of the critical current density as a function of magnetic field at the lowest measuring temperature of $T = 0.44$ K is shown in figure 10. The critical current

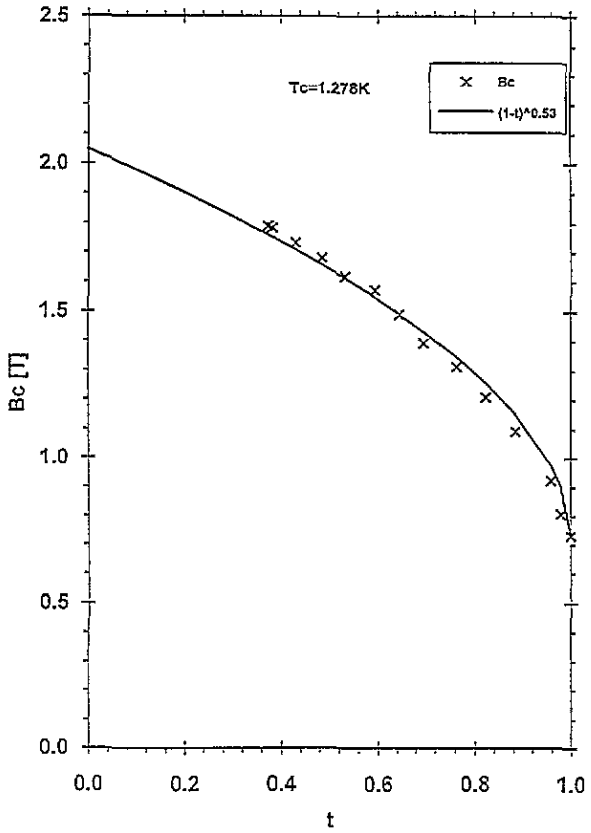

Figure 11. The critical field versus the reduced temperature $t = T/T_c$ where $T_c = 1.28$ K for the 51.2% Al film. The solid line is obtained from the Alexander expression describing percolation clusters where $B_c(T) \propto (1-t)^{0.53}$. Note that the critical field does not fall to zero at $T = T_c$ owing to the strong presence of superconducting fluctuations in the film above T_c.

density continuously decreases with increasing magnetic field. According to (6), the lengths of the links or dangling bonds are so long ($\simeq$ 17 000 Å) that it is doubtful whether many of these links or dangling bonds are electrically connected to one another. The majority of the current is carried only by a few backbones (infinite clusters) that contain tunnelling junctions. Therefore, the Peterson–Ekin model should only contribute to $J_c(B)$. We fit (5) to the $J_c(B)$ data of the 51.2% Al film using the following fitting parameters: $B_{min} = 0.006$ T, $B_{peak} = 0.025$ T, and $B_{max} = 0.059$ T. The fit is quite acceptable, as illustrated in figure 10. For this 51.2% Al film, B_{peak} is ten times larger than the B_{peak} value used in fitting the 62.4% Al film data. As the effective junction area scales inversely with B_{peak}, it is not surprising that the cross sectional areas of the backbones in the 51.2% Al film located just above the MIT are much smaller than those in the more metallic 62.4% Al film.

The critical field data, B_c, for the 51.2% Al film as a function of reduced temperature are shown in figure 11 and can be described by the Alexander prediction that $B_c(T) \propto (1-t)^{0.53}$ for a percolation structure, using $T_c = 1.278$ K [20]. The critical current density at zero field, $J_c(B = 0)$, as a function of reduced temperature is shown in figure 12. Not surprisingly, the Ambegaokar and Baratoff expression for the critical current in a tunnel junction (2) describes the temperature dependence quite satisfactorily [14]. We have used the tabulated

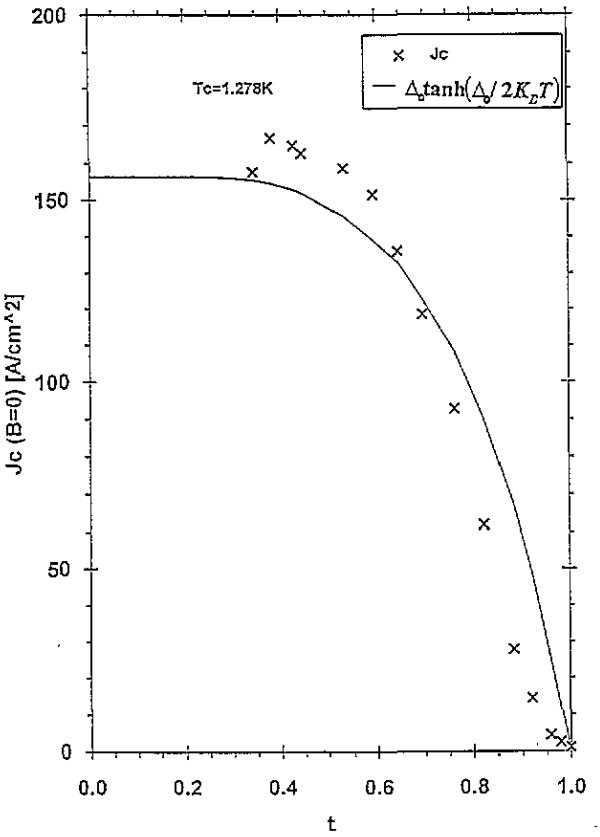

Figure 12. The critical current density $J_c(B = 0)$ at zero magnetic field as a function of reduced temperature $t = T/T_c$ where $T_c = 1.278$ K for the 51.2% Al film. The solid line is a fit using the Ambegaokar and Baratoff expression for $I_c(B = 0)$ for a tunnel junction (2).

values of the BCS energy gap $\Delta_0(T)$ given by Muhlschlegel in evaluating (2) [34].

Films in the 58% Al concentration region displayed pseudo-plateaus exhibiting very weak decreasing dependences of the critical current upon an increasing magnetic field. This behaviour could be well described by again summing the two contributions.

Values for the diffusion constant D_{diff} can be extracted from the critical field versus T curves using the expression $D_{\text{diff}} = -4k_B/[\pi e|\mathrm{d}B/\mathrm{d}T|_{T_c}]$. D_{diff} ranged from 0.2 cm^2 s^{-1} for films located just above the MIT to 1.4 cm^2 s^{-1} for the most metallic film (62.4% Al).

We now examine the dependence of the critical current density in zero field $J_c(B = 0)$ on Al volume fraction ϕ for the different metallic films in series 9. This dependence is illustrated in figure 13. Percolation theory suggests that $J_c(B = 0) \propto (\phi - \phi_c)^{1.78}$ [10, 21]. There is little tendency for the series 9 data to follow this behaviour as shown by the solid line in figure 13. Note in figure 13 that above 58% Al metal content, the critical current density falls to very low values. This behaviour was reproducible in three other series, so the effect cannot be attributed to poor-quality films. We speculate that the morphology of the films changes above 58% Al from a percolation-dominated structure to that of a dirty type-II superconductor, and that the zero-field critical currents might strongly depend upon structural effects.

Our critical current results are in conflict with those reported by Deutscher and Rappaport

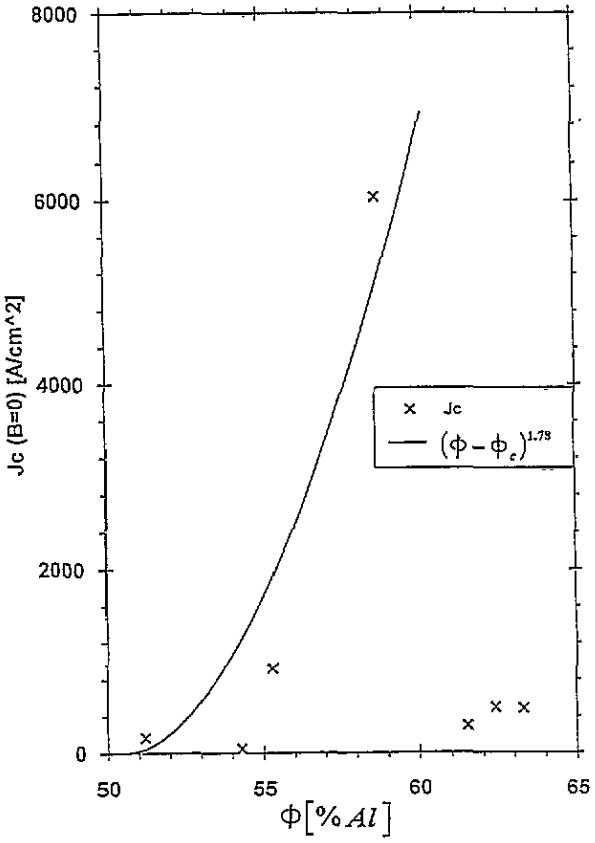

Figure 13. The dependence of the critical current density $J_c(B = 0)$ at zero magnetic field on Al volume fraction ϕ, observed in different films of series 9. The measurements were taken at $T = 0.45$ K ± 0.03 K, yielding a typical reduced temperature of $t \simeq \frac{1}{3}$. The solid line is obtained from the percolation prediction that $J_c \propto (\phi - \phi_c)^{1.78}$. For films having an Al content greater than 58% Al, the films appear to behave like dirty type-II superconductors rather than granular superconductors that can be described by percolation theory. This observation might explain the strong disagreement between theory and experiment for the 'most metallic' films, since the percolation prediction would not apply to the films having $\phi > 58\%$ Al.

on very similar 2000 Å Al–Ge films [35]. Deutscher and Rappaport made their critical current measurements at 1.4 K, stating that all their films became superconducting around 1.8 K [35]. In our series, we observed that films close to the MIT ($\phi - \phi_c < 5\%$) have transition temperatures considerably less than 1.8 K, in fact less than 1.5 K. A plot of J_c versus $(\phi - \phi_c)$ should be made with all J_c values measured at the same reduced temperature, $t = T/T_c$; it is unlikely that such a procedure was followed in [35]. To complicate matters further Hernandez *et al* have recently reported critical current measurements in thin 2D Pb films, where the critical current density exponent is expected to be 1.33, based upon the 2D discrete lattice percolation model [36]. Hernandez *et al* observed non-universal exponents ranging from 1.84 to 1.88, which they explained using either a Swiss cheese or an inverted Swiss cheese model [36]. Their experimental value of 1.85 should be compared to Deutscher and Rappaport's observed value of 1.3 obtained in a 'random' Pb–Ge 2D film [35]. At this point, we cannot explain our critical current dependence upon Al content. It is clear that

much more experimental work, including detailed morphology studies, is required on newly prepared Al–Ge granular films to resolve this disagreement.

Lastly we mention that the Lee–Stroud prediction that $1 - J_c(\text{plateau})/J_c(B = 0) \propto 1/\xi_p^2 \propto (\phi - \phi_c)^{1.78}$ is not observed experimentally for different films near the MIT [10]. This is not surprising since this derivation is based upon the assumption that, near the percolation threshold, there are numerous loops that are continuous. Experimentally, our films located near the MIT do not indicate the presence of continuous loops, since no plateaus are observed; and hence our observed fractional decrease in J_c values should not behave according to this prediction.

6. Conclusions

The initial rapid decrease of the critical current with small magnetic fields observed in all the films can be nicely described using the Peterson–Ekin model. We have observed well defined critical current plateaus in the most metallic composite Al–Ge films, whose properties can be well explained by the Lee–Stroud theory. Both processes contribute to the total critical current. At temperatures sufficiently close to T_c (that is, $T > 0.8T_c$), the plateau regions do not develop in increasing fields because the superconductivity in the links that form the loops is quenched. Metallic films very close to the MIT displayed no plateaus, only monotonic decreasing functions of $J_c(B)$ with increasing fields. Presumably, the absence of the plateaus in these films resulted from the lack of large numbers of electrically continuous and superconducting connected loops. The experimental behaviour of the J_c values in the Al–Ge films is similar to those observed in the sintered powdered YBCO samples and the Ag-sheathed Bi2223 wires. The transport processes in these high-T_c materials appear to be similar to those in the Al–Ge composite films, involving tunnelling junctions and superconducting loops having random areas.

Acknowledgments

We greatly thank Michael Slutzky for valuable assistance in running the experiments. We are grateful to Dr Yoad Yagil for sample preparation. We acknowledge Dr Mike Witcomb and his electron microscope staff of the University of Witwatersrand for the EDAX analysis results. We thank Mrs Linda Goldstein for editing the manuscript. We are indebted to the Sackler family for the purchase of the ^{3}He refrigerator. We acknowledge fruitful discussions with Professor Guy Deutscher. We gratefully thank the German–Israeli Foundation for Scientific Research and Development (GIF) and the Tel-Aviv University Internal Research Fund for financial support.

References

[1] Campbell A M and Evetts J E 1972 *Critical Currents in Superconductors* (London: Taylor and Francis) p 1
[2] Kunzler J E 1961 *Rev. Mod. Phys.* **33** 501
[3] Saint-James D, Sarma G and Thomas E J 1969 *Type II Superconductivity* (Oxford: Pergamon) p 255
[4] Tinkham M 1975 *Introduction to Superconductivity* (Tokyo: McGraw-Hill Kogakusha) p 192
[5] Peterson R L and Ekin J W 1988 *Phys. Rev.* B **37** 9848
[6] Ekin J W, Baraginski A I, Panson A J, Janocko M A, Capone D W II, Zaluzec J, Flandermeyer B, de Lima O F, Hong M, Kwo J and Liou S H 1987 *J. Appl. Phys.* **62** 4821
[7] Ekin J W, Hart H R Jr and Gaddipati A R 1990 *J. Appl. Phys.* **68** 2285

[8] Papa A R R and Altshuler E 1990 *Solid State Commun.* **76** 799
[9] Sato K, Hikata T, Mukai H, Ueyama M, Shibuta N, Kato T, Masuda T, Nagata M, Iwata K and Mitsui T 1991 *IEEE Trans. Magn.* **MAG-27** 1231
[10] Lee K H and Stroud D 1992 *Phys. Rev.* B **45** 2417
[11] Eytan G, Rosenbaum R, McLachlan D S and Albers A 1993 *Phys. Rev.* B **48** 6342
[12] McLachlan D S, Rosenbaum R, Ablers A, Eytan G, Grammatica N, Hurvits G, Pickup J and Zaken E 1993 *J. Phys.: Condens. Matter* **5** 4829
[13] Jaklevic R C, Lambe J, Silver A H and Mercereau J E 1964 *Phys. Rev. Lett.* **12** 159
[14] Ambegaokar V and Baratoff A 1963 *Phys. Rev. Lett.* **10** 486 (1963 errata **11** 104)
[15] Deutscher G, Kapitulnik A and Rappaport M 1983 *Percolation Structures and Processes* ed G Deutscher, R Zallen and J Adler (Jerusalem: Israeli Physical Society) p 207
[16] Heermann D W and Stauffer D 1981 *Z. Phys.* B **44** 339
[17] Kapitulnik A and Deutscher G 1983 *J. Phys. A: Math. Gen.* **16** L255
[18] Hoshen J, Kopelman R and Monberg E M 1978 *J. Stat. Phys.* **19** 219
[19] Lynton E A 1969 *Superconductivity* (London: Methuen) p 37
[20] Alexander S 1983 *Phys. Rev.* B **27** 1541
[21] Kirkpatrick S 1980 *Inhomogeneous Superconductors—1979* ed D U Gubser, T L Francavilla, J R Leibowitz and S A Wolf (New York: American Institute of Physics) p 79
[22] Deutscher G and Rappaport M L 1979 *J. Physique* **40** L219
[23] Deutscher G, Rappaport M and Ovadyahu Z 1978 *Solid State Commun.* **28** 593
[24] Kapitulnik A, Rappaport M L and Deutscher G 1981 *J. Physique Lett.* **42** L541
[25] Ekin J W 1989 *Appl. Phys. Lett.* **55** 905
[26] Douglass D H Jr 1961 *Phys. Rev. Lett.* **6** 346
[27] Rose-Innes A C and Rhoderick E H 1969 *Introduction to Superconductivity* (Oxford: Pergamon) p 83
[28] Gerber A, Grenet Th, Cyrot M and Beille J 1992 *Phys. Rev.* B **45** 5099
[29] Fehrenbacher R, Geshkenbein V B and Blatter G 1992 *Phys. Rev.* B **45** 5450
[30] Vinokur V M and Koshelev A E 1990 *Zh. Eksp. Teor. Fiz.* **97** 976 (Engl. transl. *Sov. Phys.–JETP* **70** 547)
[31] Larkin A I and Ovchinnikov Yu N 1979 *J. Low Temp. Phys.* **34** 409
[32] Bardeen J 1962 *Rev. Mod. Phys.* **34** 667
[33] Deutscher G 1973 *Revue Phys. Appl.* **8** 127
[34] Muhschlegel B 1959 *Z. Phys.* **155** 313
[35] Deutscher G and Rappaport M L 1979 *J. Physique* **40** L219
[36] Hernandez M C, Octavio M, Aponte J M and Rojas C 1994 *Phys. Rev.* B **49** 674
[37] Entin-Wohlman O, Kapitulnik A, Alexander S and Deutscher G 1984 *Phys. Rev.* **30** 2617
[38] Deutscher G, Entin-Wohlman O, Fishman S and Shapira Y 1980 *Phys. Rev.* **21** 5041